COMT, CRTZ, and F3'H regulate glycyrrhizic acid biosynthesis in Glycyrrhiza uralensis hairy roots

Zhixin Zhang
Beijing University of Chinese Medicine
Wenwen Ding
Beijing University of Chinese Medicine
Ziyi Chen
Beijing University of Chinese Medicine
Wenpu Xu
Beijing University of Chinese Medicine
Doudou Wang
Beijing University of Chinese Medicine
Tiangong Lu
Beijing University of Chinese Medicine
Ying Liu (liuyliwd@bucm.edu.cn)
Beijing University of Chinese Medicine https://orcid.org/0000-0002-0543-0099

Research Article

Keywords: Glycyrrhiza uralesis, COMT, CRTZ, F3'H, Gene overexpression, Gene knockout

Posted Date: April 12th, 2022

DOI: https://doi.org/10.21203/rs.3.rs-1509234/v1

Abstract

Glycyrrhiza uralensis Fisch. is prescribed as one of the original plants of licorice in *Chinese Pharmacopoeia*. This herbal medicine possesses numerous important pharmacological activities and has been used in clinic in China since ancient times. Glycyrrhizic acid (GA) is a triterpenoid compound isolated from *G. uralensis* and also one of the marker components for its quality control. Based on our pervious transcriptome study, three genes, the caffeic acid 3-O-methyltransferase gene (*COMT*), the *β*-carotene 3-hydroxylase gene (*CRTZ*), and the flavonoid 3′-monooxygenase gene (*F3′H*), were selected as our target genes due to their high correlation with GA biosynthesis. In this study, we investigated the regulatory effects of these genes on GA biosynthesis through gene editing and overexpression in *G. uralensis* hairy roots. We observed that all transgenic hairy roots were viable whether knocking out or overexpressing the three target genes, indicating that these genes had no impact on survival of hairy roots. However, compared with the wild type and negative control hairy roots, GA contents were significantly lower in hairy roots overexpressing *COMT*, *CRTZ*, and *F3′H*, while higher in those knocking out the three genes. Our findings demonstrate that the three genes, *COMT*, *CRTZ*, and *F3′H*, all negatively regulate the GA biosynthesis.

Key Messages

This study confirmed the negative regulatory effects of *COMT, CRTZ, and F3′H* on glycyrrhizic acid biosynthesis in *Glycyrrhiza uralensis*.

Introduction

Glycyrrhiza uralensis Fisch. is prescribed by *Chinese Pharmacopoeia* as one of the original plants of licorice, which is a coordinator herb in traditional Chinese medicine practice (National Pharmacopoeia Commission 2020). It is the most commonly-used Chinese herb and has been applied in the treatment of lung diseases (Chen et al. 2018) and diabetes (Yang et al. 2020) since ancient China. In recent years, increasing modern pharmacological studies have yield significant insights into this ancient Chinese herb. *G. uralensis* has been confirmed with many biological activities, such as anti-inflammatory (Huang et al. 2019; Ko et al. 2021), anti-microbial (Yang et al. 2018; Zeng et al. 2021), antiviral (Yi et al. 2022), anticancer (Jain et al. 2022; Wen et al. 2021; Xiao et al. 2011), and immunoregulatory activities (Aipire et al. 2017; Bhattacharjee et al. 2012). Abundant bioactive compounds, including triterpenoids and flavonoids, have been isolated and identified from *G. uralensis*. Among them, glycyrrhizic acid (GA), a pentacyclic triterpenoid, gradually become the most studied bioactive compound in this herb due to its excellent pharmacological activities. It has been developed into various dosage forms to treat inflammation-associated diseases in clinic (Chu et al. 2020; Xie et al. 2015). Importantly, GA is stipulated by *Chinese Pharmacopoeia* as the quality standard compound in *G. uralensis* (National Pharmacopoeia Commission 2020): medicinal materials of *G. uralensis* with a GA content ≥ 2.0% are regarded as qualified. Thus, uncovering the biosynthetic pathway of GA and elucidating the underlying regulatory mechanisms are significantly meaningful for improving the quality of this most commonly-used herb.

The biosynthesis of active ingredients is a very complicated metabolic network in *G. uralensis*. As shown in Fig. 1, the primary metabolites derived from glycolysis flow into different pathways to produce the two major bioactive components in *G. uralensis*: terpenoids and flavonoids. These pathways are crisscrossing and interacted on each other. Dimethylallyl diphosphate (DMAPP) and isopentenyl diphosphate (IPP), the common precursors of terpenoids, are synthesized through two independent and distinct pathways, the 2-C-methyl-D-erythritol 4-phosphate (MEP) pathway and the mevalonic acid (MVA) pathway (Tian et al. 2022). DMAPP and IPP for producing GA, the triterpenoid compound, are supplied by the MVA pathway (Liao et al. 2016), while the equivalent two isomeric five-carbon precursors for the synthesis of tetraterpenoids, such as *β*-carotene and zeaxanthin, are provided by the MEP pathway (Banerjee and Sharkey 2014). In addition, some primary metabolites flows into the shikimate pathway and results in the production of various flavonoids, including monolignols, flavonols, flavanones, and chalcones compounds (Vogt 2010). The above-mentioned pathways are intertwined with each other and influence the secondary metabolism in *G. uralensis*. Our previous transcriptome study demonstrated that the glycolysis, the MEP pathway, and the phenylpropanoids metabolic pathway were all tightly correlated with GA accumulation (Gao et al. 2020). We also excavated several differentially expressed genes (DEGs) from these pathways and identified their functions in succession (Wang et al. 2021). In this study, three DEGs involved in the MEP pathway and the phenylpropanoids metabolic pathway, including the *β*-carotene 3-hydroxylase gene (*CRTZ*), the caffeic acid 3-O-methyltransferase gene (*COMT*), and the flavonoid 3′-monooxygenase gene (*F3′H*), were selected and their regulatory effects on GA accumulation were evaluated.

CRTZ, a non heme 2 iron monooxygenase, is a key rate-limiting enzyme involved in the synthesis of tetraterpenoid carotenoid (Li et al. 2015). It is a multifunctional enzyme and convert *β*-carotene into *β*-cryptoxanthin and *α*-carotene into lutein (Liang et al. 2020). Current studies about CRTZ are mainly focused on its essential roles in the photoprotection and draught resistance of crops (Davison et al. 2002; Du et al. 2010). COMT mainly involves in the biosynthesis of monolignols. As a multiple-substrate enzyme, it is able to catalyze the methylation of caffealdehyde, caffeyl alcohol, caffeic acid, 5-hydroxmethylyferulic acid ester, 5-hydroxyconiferyl alcohol, and 5-hydroxyconiferaldehyde in the phenylpropanoids metabolic pathway, and eventually influences the composition of lignin (Weng et al. 2011). Several lines of evidence have confirmed that COMT plays a crucial role in the resistance to high-salt stress in higher plants (Liu et al. 2019; Zhang et al. 2019). F3′H belongs to cytochrome P450 monooxygenase family and takes part in the hydroxylation of flavonoids (Tanaka and Brugliera 2013). In *Camellia nitidissima* Chi., overexpression of *F3′H* significantly increases the contents of various polyphenol compounds (Jiang et al. 2021). It also contributes to the adaptation of *Pohlia nutans* in the south pole through the regulation of oxidation tolerance and abscisic acid sensitivity (Liu et al. 2021). To our knowledge, none of the three genes has been cloned from *G. uralensis* and their functions in secondary metabolism in *G. uralensis* are still far from clear. Our previous transcriptome study showed that the expression levels of these three genes all significantly influence GA contents in licorice (Gao et al. 2020). Hence potential roles of *CRTZ*, *COMT*, and *F3′H* on GA accumulation is worthy of study.

In the present work, we cloned *CRTZ*, *COMT*, and *F3′H* from *G. uralensis* and investigated their regulatory effects on GA biosynthesis by knocking out or overexpressing them in hairy roots. The finding of this work will provide new insights on the functions of *CRTZ*, *COMT*, and *F3′H* in the dynamic biosynthetic network of GA in *G. uralensis*.

Materials And Methods

Plant materials

Plump and healthy *G. uralensis* seeds were selected and surface-sterilized with 1% mercury bichloride and 75% ethanol solutions, and then planted on Murashige and Skoog (MS) medium for about 2 weeks. The seedlings were identified based on the internal transcribed spacer (ITS) sequences as described in our previous study (Yang et al. 2017). Next, the correct asepsis seedlings were used as materials for cloning target genes and also as explants for subsequent infection experiment.

Target genes cloning

Total RNA was extracted from the above asepsis seedlings using an All-In-One DNA/RNA Mini-Preps Kit (Sangon Biotech (Shanghai) Co., Ltd., China). cDNA was converted using a First Strand cDNA Synthesis Kit RT0212-01 (Biomiga. Inc., China). Primer pairs used for amplifying *CRTZ*, *COMT*, or *F3'H* were designed by Primer-BLAST and listed in Table S1. The PCR parameters for amplifying *COMT* were as follows: 94 °C 5 min, 35 cycles (94 °C 30 s, 52 °C 30 s, 72 °C 65 s), and 72 °C 5 min. The PCR programs for amplifying *CRTZ* were 95 °C 5 min, 35 cycles (94 °C 30 s, 54.5 °C 30 s, 72 °C 60 s), and 72 °C 5 min, and for amplifying *F3'H* were 94 °C 5 min, 35 cycles (94 °C 30 s, 52.5 °C 30 s, 72 °C 60 s), and 72 °C 5 min. The amplified fragments were cloned into pMD^{TM} 19-T Cloning Vector (Takara Biomedical Technology (Beijing) Co., Ltd., China), and sequenced by Sangon Biotech (Shanghai) Co., Ltd., China.

Construction of plant binary expression vectors and CRISPR/Cas9 vectors

We constructed plant binary expression vectors overexpressing *CRTZ*, *COMT*, or *F3'H* as shown in Fig. S1a. Three exogenous genes were inserted into pCAMBIA1305.1 at the restriction enzyme cutting sites *Spe* I and *Bgl* II, respectively. The specific primers used for amplifying target genes containing homologous sequences of pCAMBIA1305.1 are listed in Table S2. The PCR parameters were as same as those mentioned in the above section. Target genes were ligated with linearized pCAMBIA1305.1 using a BM effusion kit (Beijing Biomed Medical Technology Co., Ltd., Beijing, China) to yield recombinant plasmids, pCA-COMT, pCA-CRTZ, and pCA-F3'H. We also constructed plant CRISPR/Cas9 vectors for knocking out *CRTZ*, *COMT*, or *F3'H* as shown in Fig. S1b. The sgRNA sequences were designed and listed in Table S3. They were inserted into linearized pHSE401 at the two restriction enzyme cutting sites *Bsa* I by T4 ligase to construct the CRISPR/Cas9 plasmids, pHSE-COMT, pHSE-CRTZ, and pHSE-F3'H. The above recombinant plasmids were all electrotransfered into *Agrobacterium rhizogenes* ATCC15834. Also, the empty pCAMBIA1305.1 and pHSE401 vectors without exogenous genes were introduced into *A. rhizogenes* ATCC15834. Next, the positive colonies were selected on Tryptone-Yeast extract (TY) plates containing kanamycin (50 mg•L^{-1}). PCR and sequencing were performed to identify the correct vectors and strains.

Establishment of *G. uralensis* hairy root lines

The *G. uralensis* asepsis seedlings were cut and used as explants for inducing hairy roots. They were infected by the above recombinant *A. rhizogenes* strains as described in our previous study (Wang et al. 2021). We induced nine types of *G. uralensis* hairy roots using different recombinant *A. rhizogenes* strains. The wild type (WT) was induced by normal *A. rhizogenes* ATCC15834. The negative control hairy root lines were induced by *A. rhizogenes* strains containing empty pHSE401 or pCAMBIA1305.1, and named NC-PHSE or NC-PCA, respectively. The hairy root lines overexpressing *COMT*, *CRTZ*, or *F3'H*, which were named *COMT*$^{+}$, *CRTZ*$^{+}$, or *F3'H*$^{+}$, were induced by recombinant *A. rhizogenes* strains containing pCA-COMT, pCA-CRTZ, or pCA-F3'H, respectively. The hairy root lines knocking out *COMT*, *CRTZ*, or *F3'H*, which were named *COMT*$^{-}$, *CRTZ*$^{-}$, or *F3'H*$^{-}$, were induced by recombinant *A. rhizogenes* strains containingpHSE-COMT, pHSE-CRTZ, or pHSE-F3'H, respectively. Hairy roots were cultured on 6,7-V medium plates, and gradient concentration of cefotaxime sodium was used to eliminate the residual *A. rhizogenes*.

Identification of *G. uralensis* hairy root lines

Genomic DNA of *G. uralensis* hairy root lines were extracted by All-In-One DNA/RNA Mini-Preps Kit (Sangon Biotech (Shanghai) Co., Ltd., China) and used as PCR templates. *rol*C gene is a specific marker gene in hairy roots. We amplified *rol*C genes in all the *G. uralensis* hairy root lines as described in our previous study (Wang et al. 2021). For identification of hairy root lines *COMT*$^{+}$, *CRTZ*$^{+}$, and *F3'H*$^{+}$, we respectively amplified the corresponding target genes using the above-mentioned PCR primers (Table S1) and programs (in Section "Target genes cloning"). To analyze the gene editing sites in hairy root lines *COMT*$^{-}$, *CRTZ*$^{-}$, and *F3'H*$^{-}$, we designed specific primer pairs (Table S4) to respectively amplify the corresponding exons of *COMT*, *CRTZ*, and *F3'H*. The PCR cycling parameters were as follows: 95 °C for 5 min, 32 cycles of 95 °C for 30 s, 55.5 °C for 50 s, 72 °C for 60 s, and 72 °C for 5 min. PCR products were cloned into pMD^{TM} 19-T Cloning Vector (Takara Biomedical Technology (Beijing) Co., Ltd., China) and selected on LB plates supplemented with ampicillin (50 mg·L^{-1}). Single colonies were randomly picked for sequencing analysis which was performed by Sangon Biotech (Shanghai) Co., Ltd., China.

Gene expression levels analysis

Real-time quantitative PCR (RT-qPCR) was carried out with *β-actin* gene as the internal to analyze the expression levels of *COMT*, *CRTZ*, or *F3'H* in hairy root lines overexpressing the three target genes. Primers for RT-qPCR are listed in Table S5. Total RNA of *COMT*$^{+}$, *CRTZ*$^{+}$, and *F3'H*$^{+}$ samples were extracted and reversely transcribed into cDNA as mentioned above (in Section "Target genes cloning"). RT-qPCR was carried out using an Agilent StrataGene Mx3005P QPCR (Agilent Technologies, USA) with a program as follows: 95 ℃ 3 min, 45 cycles (95 ℃ 7 sec, 57 ℃ 10 sec, 72 ℃ 15 sec). The expression level difference was evaluated by the $2^{-\Delta\Delta Ct}$ method in triplicate (Annaratone et al. 2013).

GA content assay by UPLC

The validated hairy roots were isolated from each line and transcultured in liquid 6,7-V medium (250 mL-conical flasks, 110 rpm, 25 °C, dark). After hairy root lines adapted to the liquid culture system and thrived, the healthy branches (2.0 g) were cut in triplicate and suspension cultured in fresh medium at the same conditions for three weeks. Next, the collected hairy roots were dried at 65 °C. The UPLC method for determination of the GA contents in *G. uralensis* hairy roots established in our previous study was adopted (Wang et al. 2021). The standard compound GA with a purity of 99.45% was purchased from China National Institutes for Food and Drug Control. The stock solution of GA was prepared by 50% methanol at a concentration of 0.0904 mg·mL^{-1}. The linear was evaluated at seven points by gradient dilution of the GA stock solution to 0.09040, 0.07232, 0.05424, 0.04520, 0.01808, 0.00904, and 0.00452 mg·mL^{-1}. The chromatographic conditions were as follows: chromatographic instrument: Waters Acquity UPLC system (Waters Corporation, Miford, Massachusetts, USA), chromatographic column: Waters UPLC BEH C_{18} column (2.1 mm × 100 mm, 1.7 μm), UV detection wavelength: 250 nm, column temperature: 40 °C, flow rate: 0.3 mL·min^{-1}, and injection volume: 1 μL. The mobile phase A was acetonitrile and B was 0.05% phosphoric acid. The UPLC gradient elution program was shown in Table S6.

Statistical and bioinformatics analysis

IBM SPSS Statistics 20 was applied to perform the statistical analysis. BLAST (http://www.ncbi.nlm.nih.gov) and DNAMAN 6.0.3.99 were used to analyze the sequencing results. MEGA 11 was applied to construct the phylogenetic tree using Maximum Composite Likelihood method.

Results

Identification of three target genes

As shown in Fig. S2a, three fragments, the length of which were about 1200, 1000, and 1000 bp, were obtained by PCR. Sequencing results confirmed that the exact full length of the three PCR products were 1140, 930, and 993 bp, respectively. The 1140 bp-PCR product had 86.71% identity with the *Abrus precatorius COMT* (GenBank accession No. XM_027512828.1), the 930 bp-PCR product had 89.82 % identity with the *Glycine max CRTZ* (NM_001254504.1), and the 993 bp-PCR product had 81.82% identity with *Cajanus cajan F3'H* (XM_020357268.2), indicating the *COMT*, *CRTZ*, and *F3'H* sequences were obtained from *G. uralensis*. We registered these sequences in GenBank and got the accession numbers as follows: *COMT* (MZ169549), *CRTZ* (MZ169550), and *F3'H* (MZ169551). It is the very first time to identify *COMT*, *CRTZ*, and *F3'H* from *G. uralensis.* To evaluate the evolution of these genes, we then established phylogenetic trees based on COMT, CRTZ, and F3'H homologous sequences registered in NCBI, respectively. As shown in Fig. 2, COMT and F3'H homologous sequences both clustered into three major independent clades, Dicotyledoneae, Monocotyledoneae, and Pteridophyta, while CRTZ orthologs clustered into four, Dicotyledoneae, Monocotyledoneae, Pteridophyta, and Bryophyta. These findings suggest that the evolution of the three enzymes is stable and corresponding to the evolution of species.

Construction of recombinant vectors

As shown in Fig. S2b, three fragmentswere amplified from the plant binary expression vectors, pCA-COMT, pCA-CRTZ, and pCA-F3'H, respectively. Sequencing results further confirmed that these PCR products were completely identified with *COMT* (MZ169549), *CRTZ* (MZ169550), and *F3'H* (MZ169551)that we cloned from *G. uralensis*. These findings demonstrated that the plant binary expression vectors for overexpressing *COMT*, *CRTZ*, or *F3'H* were correct. As shown in Fig. S2c, several 400 bp PCR products were obtained from the plant CRISPR/Cas9 vectors, pHSE-COMT, pHSE-CRTZ, and pHSE-F3'H. Sequencing results confirmed that these fragments contained the corresponding sgRNA sequences of target genes, indicating that the CRISPR/Cas9 vectors for knocking out *COMT*, *CRTZ*, or *F3'H* were constructed successfully.

Identification of *G. uralensis* hairy root lines

We generated nine types of *G. uralensis* hairy root lines, including WT, NC-PCA, NC-PHSE, *COMT*$^{+}$, *CRTZ*$^{+}$, *F3'H*$^{+}$, *COMT*$^{-}$, *CRTZ*$^{-}$, and *F3'H*$^{-}$. Fig. 3 shows the growth situation of these hairy roots after the onset of induction for 10, 20, and 30 days. They all grew in good condition. To identify these hairy root lines, we firstly cloned the *rol*C genes, the signature gene in hairy roots, from all samples and got 600 bp-fragments by PCR (Fig. S3a), which were identified to have 100% identity with *rol*C (GenBank accession No. DQ160187.1). Also, the fragments amplified from *COMT*$^{+}$, *CRTZ*$^{+}$, and *F3'H*$^{+}$ showing in Fig. S3b were confirmed with correct sequences. Fig. S3c and S3d exhibit the third exons of *COMT* and *CRTZ*amplified from *COMT*$^{-}$ and *CRTZ*$^{-}$ respectively, and Fig. S3e shows the first exons of *F3'H* amplified from *F3'H*$^{-}$. These fragments, as described in next section, will be used to analyze the exact editing sites of target genes in hairy root lines *COMT*$^{-}$, *CRTZ*$^{-}$, and *F3'H*$^{-}$ through further cloning and sequencing. In the end, one WT, five *COMT*$^{+}$, five *CRTZ*$^{+}$, seven *F3'H*$^{+}$, three *COMT*$^{-}$, five *CRTZ*$^{-}$, four *F3'H*$^{-}$,one NC-PCA, and one NC-PHSE samples were obtained.

Characterization of gene knockout and overexpression in transgenic *G. uralensis* hairy root lines

Further cloning and sequencing analysis confirmed that the *COMT* gene was edited in four hairy root lines (*COMT*$^{-}$-2,-5,-6, and -8) out of nine with a gene editing efficiency of 44.4%. The gene editing details are shown in Fig. 4a and the mutation sites present in COMT amino acid sequences are listed in Table 1. We observed that the synonymous mutation appears in *COMT*$^{-}$-2, while the missense mutations present in the other three samples. The most efficient gene edition was a fragment deletion in *COMT*$^{-}$-5, which results in a termination codon "TAA" in this position. *CRTZ* gene was edited in eight lines (*CRTZ*$^{-}$-1, -2,-3,-4,-5,-6,7, and-8) out of ten with an editing efficiency of 80%. Among them, homozygous mutations were present in four samples, *CRTZ*$^{-}$-1,-3,-4 and-6 (Fig. 4b), while heterozygous mutations in the other four (Fig. S4a). Frameshifts were observed in all lines. The mutation sites in CRTZ amino acid sequences are listed in Table 2. *CRTZ*$^{-}$-1 and *CRTZ*$^{-}$-6 exhibit the same two mutation sites, while *CRTZ*$^{-}$-3 and *CRTZ*$^{-}$-4 share a similar one mutation site in CRTZ sequences. All mutation sites in these four samples were located within the functional domain of CRTZ. Further cloning and sequencing analysis showed that *F3'H* gene was edited in seven lines (*F3'H*$^{-}$-2, -4, -5, -7, -8, -9, and -10) out of eleven with a gene editing efficiency of 63.6%. Four hairy root lines, *F3'H*$^{-}$-2, -7, -8, and -10, were

confirmed with homozygous mutations (Fig. 4c), while the other three lines were heterozygous mutations (Fig. S4b). The mutation sites present in F3'H amino acid sequences are listed in Table 3. *F3'H*-2 and *F3'H*-10 exhibit 16 similar mutation sites in F3'H sequences. All these mutations are located within the functional domain of F3'H. We next examined the gene expression levels of the three target genes in newly constructed *COMT*$^+$, *CRTZ*$^+$, and *F3'H*$^+$ hairy root lines. As illustrated in Fig. 4d, the relative expression levels of *COMT*, *CRTZ*, and *F3'H* in *COMT*$^+$, *CRTZ*$^+$, and *F3'H*$^+$ hairy root lineswere all sharply higher than that in WT. In particular, samples *COMT*$^+$-4, *CRTZ*$^+$-4, and *F3'H*$^+$-6 showed the highest expression level in their respective groups.

GA content assay by UPLC in *G. uralensis* hairy root samples

Fig. 5a shows the healthy and luxuriant hairy root samples cultured in liquid 6,7-V medium. Fig. 5b shows the collected hairy root samples, which were prepared for UPLC analysis. It is worth noting that samples *F3'H*$^-$ and *CRTZ*$^+$ look partial white and *CRTZ*$^-$ looks reddish, although most of the hairy root lines are yellowish white. The UPLC chromatograms of reference substance GA, WT, NC-PCA, NC-PHSE, *COMT*$^+$, *CRTZ*$^+$, *F3'H*$^+$, *COMT*$^-$, *CRTZ*$^-$, and *F3'H*$^-$ are shown in Fig. 6a. The UPLC retention time of GA was 6.532 min, and the standard curve was as follows: Y = 2,683,455.37 X - 1,660.17 (R^2 = 0.9999). The GA contents in all of the hairy root samples are calculated and listed in Table 4. The difference of GA content among samples is shown in Fig. 6b and which among groups is shown in Fig. 6c. We found that the GA contents in negative control (NC-PCA and NC-PHSE) were equivalent to that in WT and no significance were detected among these samples. Interestingly, we noticed that gene expression levels of the three target genes exhibit negative correlations to GA contents in hairy root samples when comparing to WT and negative control. For example, the GA contents in all the seven *F3'H*$^+$ samples were all significantly lower than that in WT and NC-PCA, and which in three *F3'H*$^-$ samples (*F3'H*-2, -8, and -10) were all remarkably higher than that in WT and NC-PHSE. In group *F3'H*$^-$, the only exception was *F3'H*-7, the GA content in which was higher than that in WT and NC-PHSE, but the difference was not significant. The similar results were also observed in *COMT*$^+$, *CRTZ*$^+$, *COMT*$^-$, and *CRTZ*$^-$ samples. Next, we analyzed the GA content difference among groups (Table 4) and found that the GA contents in groups *F3'H*$^+$ (average value: 2.3654 mg·g^{-1}), *CRTZ*$^+$ (2.2050 mg·g^{-1}), and *COMT*$^+$ (2.3509 mg·g^{-1}) were significantly lower than that in both WT (3.3242 mg·g^{-1}) and NC-PCA (3.5188 mg·g^{-1}). While, the GA contents in groups *F3'H*$^-$ (5.4744 mg·g^{-1}), *CRTZ*$^-$ (5.3651 mg·g^{-1}) and *COMT*$^-$ (4.2746 mg·g^{-1}) were significantly higher than that in WT as well as NC-PHSE (3.3459 mg·g^{-1}). These findings suggest that the expression of three target genes negatively correlates to GA production.

Discussion And Conclusion

In recent years, suspension hairy root systems have been applied to produce valuable effective components (Chen et al. 2018; Sim et al. 1994; Srivastava and Srivastava 2007) and investigate the secondary metabolism pathways in various medicinal plants (Huber et al. 2009; Ma et al. 2015; Shi et al. 2019). Increasing lines of evidence have confirmed that overexpression or knockout of functional genes is able to modulate the secondary metabolism and consequently increase the active components contents in medicinal plants (Li et al. 2017; Zhou et al. 2021). Similar research has also been carried out in *G. uralensis*, the most commonly-used Chinese herb. In the past several years, our previous studies identified more than ten functional genes involved in the biosynthetic pathways of triterpenoids and flavonoids in *G. uralensis*. We confirmed that overexpressing or knocking out *β*-amyrin synthase (*β*-AS), UDP-Galactose/Glucose-4-epimerase (UGE), auxin-responsive protein IAA (ARPI), chalcone isomerase (CHI), chalcone synthase (CHS) genes, and several other genes did regulate the production of active components in *G. uralensis* hairy roots (Hou et al. 2021; Wang et al. 2021; Yin et al. 2020). Therefore, hairy root system is a well-established model to investigate the secondary metabolism and the underlying mechanism in *G. uralensis*.

In the present study, we established transgenic *G. uralensis* hairy root lines to overexpress or knock out three functional genes, *CRTZ*, *COMT*, and *F3'H*, through *A. rhizogenes*-mediated method. We obtained five *COMT*$^+$, five *CRTZ*$^+$, seven *F3'H*$^+$, three *COMT*$^-$, five *CRTZ*$^-$, and four *F3'H*$^-$ samples in total. Also, we induced WT and negative control hairy root samples, including NC-PHSE and NC-PCA. We found that all the hairy roots were ramulous and exuberant indicating that the overexpression or knockout of the three genes had no effects on the generation or development of *G. uralensis* hairy roots. Interestingly, we also noticed that most of the hairy roots were normally yellowish white, however, the colors of *F3'H*$^-$, *CRTZ*$^+$, and *CRTZ*$^-$ present differently. *F3'H*$^-$ and *CRTZ*$^+$ were relatively light, while *CRTZ*$^-$ was reddish. It has been reported that *F3'H* gene is involved in the synthesis of anthocyanin and which results in the color change in soybean hairy roots (Fan et al. 2020). We speculate that the pale color of *F3'H*$^-$ is due to the same reason and will investigate the underlying molecular mechanism in future study. CRTZ is the key enzyme involved in the synthesis of carotenoid. Generally, overexpression of *CRTZ* contributes to the decomposition of *β*-carotene (Pollmann et al. 2017), while knockout of *CRTZ* leads to the accumulation of *β*-carotene (Tomlekova et al. 2021). It has been observed in *Brassica rapa* and *Oncidium hybridum* that the accumulation of *β*-carotene caused by the down-regulation of *CRTZ* makes the flower color turn from yellow to orange (Chiou et al. 2010; Zhang et al. 2019). These researches could be a possible explanation to our study that the color of *CRTZ*$^+$ looks partial white, whereas the color of *CRTZ*$^-$ looks reddish.

By UPLC analysis, we found that compared with WT and negative control, the GA contents in hairy root groups overexpressing the three target genes were all significantly lower while that in groups knocking out these genes were higher, indicating negative regulatory effects of *CRTZ*, *COMT*, and *F3'H* on GA biosynthesis. As described above, CRTZ is an essential rate-limiting enzyme involved in the synthesis of tetraterpenoid carotenoid (Li et al. 2015). Generally, IPP and DMAPP for tetraterpenoid production are provided by the MEP pathway, while which for triterpenoid production are supplied by the MVA pathway. Although the two pathways are independent and take place in different cellular localization, the MEP pathway occurs in plastids while the MVA pathway in cytoplasm (Tian et al. 2022), the two isomeric five-carbon precursors produced by the two pathways can translocate between plastids and cytoplasm (Hemmerlin et al. 2012). Thus, the triterpenoid saponins can be synthesized by the MEP pathway in *Panax japonicus* (Xu et al. 2020). In this study, knocking out *CRTZ* increases while expressing *CRTZ* decreases the GA contents in *G. uralensis* hairy roots also suggests a close relationship between the MVA and MEP pathways. We speculate that knocking out *CRTZ* blocks the conversion from *β*-carotene to *β*-cryptoxanthin and results in the accumulation of *β*-carotene, which causes a feedback inhibition of the MEP pathway. Hence the carbon source flowing into the MVA pathway increases and leads to the

production of GA. In addition, the excess accumulation of β-carotene promotes IPP and DMAPP to translocate from plastids to cytoplasm, which also supplies more substrates for the synthesis of GA. Thus, *CRTZ* negatively regulates the biosynthesis of GA.

COMT is a key enzyme involved in the biosynthesis of monolignols (Saluja et al. 2021). Knocking out *COMT* causes a sharp decrease of S-lignin level and changes the ratio between the S- and G-lignin, which then influences the transcriptional levels of stress response genes in higher plants (Gallego-Giraldo et al. 2018; Guo et al. 2001). Since triterpenoids, such as GA, is essential in plant stress response (Shirazi et al. 2019), we suppose that the transcriptional level changes of stress response genes caused by the knockout or overexpression of *COMT* may supply a reason for the change of GA contents observed in the *G. uralensis* hairy roots. Moreover, COMT has also been reported to play an important role in the synthesis of melatonin in plants (Zhang et al. 2021). For example, overexpressing *COMT* promotes the synthesis of melatonin and subsequently increases the content of diterpenoid compound gibberellin in *Arabidopsis thaliana* (Yang et al. 2019). Therefore, we speculate that the overexpression of *COMT* also upregulates the diterpenoids synthesis genes in *G. uralensis*, which increases the carbon source flowing to the MEP pathway and decreases that to the MVA pathway. Thus, overexpressing *COMT* reduces whereas knocking out *COMT* promotes GA accumulation.

F3'H is a key enzyme involved in the biosynthesis of flavonols (Tanaka and Brugliera 2013). Previous studies have confirmed that several cytochrome P450 monooxygenases, such as CYP716A53v2 and CYP716A47, play an essential role in triterpenoids biosynthesis (Han et al. 2012; Han et al. 2011). However, no studies have been reported about the regulatory effects of *F3'H* on triterpenoids production so far. In this study, we confirmed a negative regulatory effect of *F3'H* on GA accumulation. As shown in Fig. 1, triterpenoids and flavonoids are the main secondary metabolites in *G. uralensis*. The synthesis of them need to competitively use the primary metabolites. We hypothesize that knocking out *F3'H* causes an inhibitory effect on the biosynthesis of flavonols in *G. uralensis*, hence leads to a decrease of phosphoenolpyruvate flowing into the phenylpropanoids metabolic pathway, which promotes the production of acetyl-CoA, the substrate of the MVA pathway. Therefore, the knockout of *F3'H* increases the GA accumulation in *G. uralensis*.

To sum up, our results demonstrate that *CRTZ*, *COMT*, and *F3'H* all negatively regulate the GA biosynthesis. In the future, we will continue investigate the regulatory effects and the underlying mechanisms of other functional genes in GA biosynthesis and establish the gene regulatory network responsible for secondary metabolism in *G. uralensis*.

Abbreviations

ARPI, Auxin-responsive protein IAA; ***β*-AS**, *β*-amyrin synthase; **CHI**, Chalcone isomerase; **CHS**, Chalcone synthase; ***COMT***, Caffeic acid 3-O-methyltransferase gene; ***CRTZ***, *β*-carotene 3-hydroxylase gene; **DEGs**, Differentially expressed genes; **DMAPP**, Dimethylallyl diphosphate; ***F3'H***, Flavonoid 3'-monooxygenase gene; **GA**, Glycyrrhizic acid; **IDI**: Isopentenyl diphosphate isomerase; **IPP**, Isopentenyl diphosphate; **ITS**, Internal transcribed spacer; **M**, Missense mutations; **MEP**, 2-C-methyl-D-erythritol 4-phosphate; **MS**, Murashige and Skoog; **MVA**, Mevalonic acid; **RT-qPCR**, Real-time quantitative PCR; **S**, Synonymous mutations; **TY**, Tryptone-Yeast extract; **UGE**, UDP-Galactose/Glucose-4-epimerase; **WT**, Wild type

Declarations

Funding: Not applicable.

Conflicts of interest: The authors declare that there is no conflict of interest regarding the publication of this paper.

Availability of data and material: Not applicable.

Code availability: Not applicable.

Authors' contributions: YL conceived and designed the experiments. ZXZ, WWD and ZYC performed the experiments. WPX and DDW helped in analyzing the relevant data and searching literature. YL and TGL wrote the manuscript.

Ethics approval: Not applicable.

Consent to participate: Not applicable.

Consent for publication: Not applicable.

References

1. Aipire A, Li JY, Yuan PF, He J, Hu YL, Liu L, Feng XL, Li YJ, Zhang FC, Yang JH, Li JY (2017) *Glycyrrhiza uralensis* water extract enhances dendritic cell maturation and antitumor efficacy of HPV dendritic cell-based vaccine. Sci Rep 7:43796. https://doi.org/10.1038/srep43796
2. Annaratone L, Volante M, Asioli S, Rangel N, Bussolati G (2013) Characterization of neuroendocrine tumors of the pancreas by real-time quantitative polymerase chain reaction. A methodological approach. Endocr Pathol 24:83-91. https://doi.org/10.1007/s12022-013-9246-y
3. Banerjee A, Sharkey TD (2014) Methylerythritol 4-phosphate (MEP) pathway metabolic regulation. Nat Prod Rep 31:1043-1055. https://doi.org/10.1039/c3np70124g
4. Bhattacharjee S, Bhattacharjee A, Majumder S, Majumdar SB, Majumdar S (2012) Glycyrrhizic acid suppresses Cox-2-mediated anti-inflammatory responses during *Leishmania donovani* infection. J Antimicrob Chemother 67:1905-1914. https://doi.org/10.1093/jac/dks159
5. Chen CL, Shenoy AK, Padia R, Fang DD, Jing Q, Yang P, Su SB, Huang S (2018) Suppression of lung cancer progression by isoliquiritigenin through its metabolite 2, 4, 2', 4'-Tetrahydroxychalcone. J Exp Clin Cancer Res 37:243. https://doi.org/10.1186/s13046-018-0902-4

6. Chen IJ, Lee MS, Lin MK, Ko CY, Chang WT (2018) Blue light decreases tanshinone IIA content in Salvia miltiorrhiza hairy roots via genes regulation. J Photochem Photobiol B 183:164-171. https://doi.org/10.1016/j.jphotobiol.2018.04.013
7. Chiou CY, Pan HA, Chuang YN, Yeh KW (2010) Differential expression of carotenoid-related genes determines diversified carotenoid coloration in floral tissues of *Oncidium* cultivars. Planta 232:937-948. https://doi.org/10.1007/s00425-010-1222-x
8. Chu SF, Niu ZQ, Guo QX, Bi HZ, Li XY, Li FF, Zhang Z, He WB, Cao P, Chen NH, Sun XY (2020) Combination of monoammonium glycyrrhizinate and cysteine hydrochloride ameliorated lipopolysaccharide/galactosamine-induced acute liver injury through Nrf2/ARE pathway. Eur J Pharmacol 882:173258. https://doi.org/10.1016/j.ejphar.2020.173258
9. Davison PA, Hunter CN, Horton P (2002) Overexpression of beta-carotene hydroxylase enhances stress tolerance in *Arabidopsis*. Nature 418:203-206. https://doi.org/10.1038/nature00861
10. Du H, Wang NL, Cui F, Li XH, Xiao JH, Xiong LZ (2010) Characterization of the beta-carotene hydroxylase gene *DSM2* conferring drought and oxidative stress resistance by increasing xanthophylls and abscisic acid synthesis in rice. Plant Physiol 154:1304-1318. https://doi.org/10.1104/pp.110.163741
11. Fan YL, Wang XY, Li HY, Liu S, Jin LS, Lyu YY, Shi MD, Liu SR, Yang XY, Lyu SH (2020) Anthocyanin, a novel and user-friendly reporter for convenient, non-destructive, low cost, directly visual selection of transgenic hairy roots in the study of rhizobia-legume symbiosis. Plant Methods 16:94. https://doi.org/10.1186/s13007-020-00638-w
12. Gallego-Giraldo L, Pose S, Pattathil S, Peralta AG, Hahn MG, Ayre BG, Sunuwar J, Hernandez J, Patel M, Shah J, Rao XL, Knox JP, Dixon RA (2018) Elicitors and defense gene induction in plants with altered lignin compositions. New Phytol 219:1235-1251. https://doi.org/10.1111/nph.15258
13. Gao ZQ, Tian SK, Hou JM, Zhang ZX, Yang L, Hu T, Li WD, Liu Y (2020) RNA-Seq based transcriptome analysis reveals the molecular mechanism of triterpenoid biosynthesis in *Glycyrrhiza glabra*. Bioorg Med Chem Lett 30:127102. https://doi.org/10.1016/j.bmcl.2020.127102
14. Guo DJ, Chen F, Inoue K, Blount JW, Dixon RA (2001) Downregulation of caffeic acid 3-*O*-methyltransferase and caffeoyl CoA 3-*O*-methyltransferase in transgenic alfalfa: impacts on lignin structure and implications for the biosynthesis of G and S lignin. Plant Cell 13:73-88. https://doi.org/10.1105/tpc.13.1.73
15. Han JY, Hwang HS, Choi SW, Kim HJ, Choi YE (2012) Cytochrome P450 *CYP716A53v2* catalyzes the formation of protopanaxatriol from protopanaxadiol during ginsenoside biosynthesis in *Panax ginseng*. Plant Cell Physiol 53:1535-1545. https://doi.org/10.1093/pcp/pcs106
16. Han JY, Kim HJ, Kwon YS, Choi YE (2011) The Cyt P450 enzyme CYP716A47 catalyzes the formation of protopanaxadiol from dammarenediol-II during ginsenoside biosynthesis in *Panax ginseng*. Plant Cell Physiol 52:2062-2073. https://doi.org/10.1093/pcp/pcr150
17. Hemmerlin A, Harwood JL, Bach TJ (2012) A raison d'etre for two distinct pathways in the early steps of plant isoprenoid biosynthesis? Prog Lipid Res 51:95-148. https://doi.org/10.1016/j.plipres.2011.12.001
18. Hou JM, Tian SK, Yang L, Zhang ZX, Liu Y (2021) A systematic review of the Uridine diphosphate-Galactose/Glucose-4-epimerase (UGE) in plants. Plant Growth Regul 93:267-278. https://doi.org/10.1007/s10725-020-00686-1
19. Huang WC, Liu CY, Shen SC, Chen LC, Yeh KW, Liu SH, Liou CJ (2019) Protective Effects of Licochalcone A Improve Airway Hyper-Responsiveness and Oxidative Stress in a Mouse Model of Asthma. Cells 8:10.3390/cells8060617
20. Huber C, Bartha B, Harpaintner R, Schroder P (2009) Metabolism of acetaminophen (paracetamol) in plants–two independent pathways result in the formation of a glutathione and a glucose conjugate. Environ Sci Pollut Res Int 16:206-213. https://doi.org/10.1007/s11356-008-0095-z
21. Jain R, Hussein MA, Pierce S, Martens C, Shahagadkar P, Munirathinam G (2022) Oncopreventive and oncotherapeutic potential of licorice triterpenoid compound glycyrrhizin and its derivatives: Molecular insights. Pharmacol Res 178:106138. https://doi.org/10.1016/j.phrs.2022.106138
22. Jiang LN, Fan ZQ, Tong R, Yin HF, Li JY, Zhou XW (2021) Flavonoid 3'-hydroxylase of *Camellia nitidissima* Chi. promotes the synthesis of polyphenols better than flavonoids. Mol Biol Rep 48:3903-3912. https://doi.org/10.1007/s11033-021-06345-6
23. Ko HM, Lee SH, Jee W, Jung JH, Kim KI, Jung HJ, Jang HJ (2021) Gancaonin N from *Glycyrrhiza uralensis* attenuates the inflammatory response by downregulating the NF-kappaB/MAPK pathway on an acute pneumonia in vitro model. Pharmaceutics 13:10.3390/pharmaceutics13071028
24. Li B, Cui GH, Shen GA, Zhan ZL, Huang LQ, Chen JC, Qi XQ (2017) Targeted mutagenesis in the medicinal plant *Salvia miltiorrhiza*. Sci Rep 7:43320. https://doi.org/10.1038/srep43320
25. Li XR, Tian GQ, Shen HJ, Liu JZ (2015) Metabolic engineering of *Escherichia coli* to produce zeaxanthin. J Ind Microbiol Biotechnol 42:627-636. https://doi.org/10.1007/s10295-014-1565-6
26. Liang MH, Xie H, Chen HH, Liang ZC, Jiang JG (2020) Functional identification of two types of carotene hydroxylases from the green alga Dunaliella bardawil rich in lutein. ACS Synth Biol 9:1246-1253. https://doi.org/10.1021/acssynbio.0c00070
27. Liao P, Hemmerlin A, Bach TJ, Chye ML (2016) The potential of the mevalonate pathway for enhanced isoprenoid production. Biotechnol Adv 34:697-713. https://doi.org/10.1016/j.biotechadv.2016.03.005
28. Liu DD, Sun XS, Liu L, Shi HD, Chen SY, Zhao DK (2019) Overexpression of the Melatonin Synthesis-Related Gene SlCOMT1 Improves the Resistance of Tomato to Salt Stress. Molecules 24:10.3390/molecules24081514
29. Liu HW, Liu SH, Wang HJ, Chen KS, Zhang PY (2021) The flavonoid 3'-hydroxylase gene from the Antarctic moss *Pohlia nutans* is involved in regulating oxidative and salt stress tolerance. Biotechnol Appl Biochem 10.1002/bab.2143
30. Ma XH, Ma Y, Tang JF, He YL, Liu YC, Ma XJ, Shen Y, Cui GH, Lin HX, Rong QX, Guo J, Huang LQ (2015) The biosynthetic pathways of Tanshinones and Phenolic acids in *Salvia miltiorrhiza*. Molecules 20:16235-16254. https://doi.org/10.3390/molecules200916235
31. National Pharmacopoeia Commission (2020) Chinese Pharmacopoeia, 2020 edn. China Medical Science and Technology Press, Beijing, pp 88-89
32. Pollmann H, Breitenbach J, Sandmann G (2017) Engineering of the carotenoid pathway in *Xanthophyllomyces dendrorhous* leading to the synthesis of zeaxanthin. Appl Microbiol Biotechnol 101:103-111. https://doi.org/10.1007/s00253-016-7769-0

33. Saluja M, Zhu FY, Yu HF, Walia H, Sattler SE (2021) Loss of COMT activity reduces lateral root formation and alters the response to water limitation in sorghum *brown midrib (bmr) 12* mutant. New Phytol 229:2780-2794. https://doi.org/10.1111/nph.17051
34. Shi M, Huang FF, Deng CP, Wang Y, Kai GY (2019) Bioactivities, biosynthesis and biotechnological production of phenolic acids in Salvia miltiorrhiza. Crit Rev Food Sci Nutr 59:953-964. https://doi.org/10.1080/10408398.2018.1474170
35. Shirazi Z, Aalami A, Tohidfar M, Sohani MM (2019) Triterpenoid gene expression and phytochemical content in Iranian licorice under salinity stress. Protoplasma 256:827-837. https://doi.org/10.1007/s00709-018-01340-4
36. Sim SJ, Kim DJ, Chang HN (1994) Shikonin production by extractive cultivation in transformed-suspension and hairy root cultures of *Lithospermum erythrorhizon*. Ann N Y Acad Sci 745:442-454. https://doi.org/10.1111/j.1749-6632.1994.tb44395.x
37. Srivastava S, Srivastava AK (2007) Hairy root culture for mass-production of high-value secondary metabolites. Crit Rev Biotechnol 27:29-43. https://doi.org/10.1080/07388550601173918
38. Tanaka Y, Brugliera F (2013) Flower colour and cytochromes P450. Philos Trans R Soc Lond B Biol Sci 368:20120432. https://doi.org/10.1098/rstb.2012.0432
39. Tian SK, Wang DD, Yang L, Zhang ZX, Liu Y (2022) A systematic review of 1-Deoxy-D-xylulose-5-phosphate synthase in terpenoid biosynthesis in plants. Plant Growth Regul 96:221-235. https://doi.org/10.1007/s10725-021-00784-8
40. Tomlekova N, Spasova-Apostolova V, Pantchev I, Sarsu F (2021) Mutation Associated with Orange Fruit Color Increases Concentrations of beta-Carotene in a Sweet Pepper Variety (*Capsicum annuum* L.). Foods 10:10.3390/foods10061225
41. Vogt T (2010) Phenylpropanoid biosynthesis. Mol Plant 3:2-20. https://doi.org/10.1093/mp/ssp106
42. Wang DD, Zhang ZX, Yang L, Tian SK, Liu Y (2021) *ARPI*, beta-*AS*, and *UGE* regulate glycyrrhizin biosynthesis in *Glycyrrhiza uralensis* hairy roots. Plant Cell Rep 40:1285-1296. https://doi.org/10.1007/s00299-021-02712-6
43. Wen Y, Chen HS, Zhang L, Wu ML, Zhang F, Yang D, Shen JG, Chen JP (2021) Glycyrrhetinic acid induces oxidative/nitrative stress and drives ferroptosis through activating NADPH oxidases and iNOS, and depriving glutathione in triple-negative breast cancer cells. Free Radic Biol Med 173:41-51. https://doi.org/10.1016/j.freeradbiomed.2021.07.019
44. Weng JK, Akiyama T, Ralph J, Chapple C (2011) Independent recruitment of an O-methyltransferase for syringyl lignin biosynthesis in Selaginella moellendorffii. Plant Cell 23:2708-2724. https://doi.org/10.1105/tpc.110.081547
45. Xiao XY, Hao M, Yang XY, Ba Q, Li M, Ni SJ, Wang LS, Du X (2011) Licochalcone A inhibits growth of gastric cancer cells by arresting cell cycle progression and inducing apoptosis. Cancer Lett 302:69-75. https://doi.org/10.1016/j.canlet.2010.12.016
46. Xie CF, Li XT, Wu JS, Liang ZF, Deng FF, Xie W, Zhu MM, Zhu JY, Zhu WW, Geng SS, Zhong CY (2015) Anti-inflammatory Activity of Magnesium Isoglycyrrhizinate Through Inhibition of Phospholipase A2/Arachidonic Acid Pathway. Inflammation 38:1639-1648. https://doi.org/10.1007/s10753-015-0140-2
47. Xu R, Zhang J, You JM, Gao LM, Li YC, Zhang SP, Zhu WJ, Shu SH, Xiong C, Xiong H, Chen P, Guo J, Liu ZG (2020) Full-length transcriptome sequencing and modular organization analysis of oleanolic acid- and dammarane-type saponins related gene expression patterns in Panax japonicus. Genomics 112:4137-4147. https://doi.org/10.1016/j.ygeno.2020.06.045
48. Yang G, Lee HE, Yeon SH, Kang HC, Cho YY, Lee HS, Zouboulis CC, Han SH, Lee JH, Lee JY (2018) Licochalcone A attenuates acne symptoms mediated by suppression of NLRP3 inflammasome. Phytother Res 32:2551-2559. https://doi.org/10.1002/ptr.6195
49. Yang L, Jiang Y, Zhang ZX, Hou JM, Tian SK, Liu Y (2020) The anti-diabetic activity of licorice, a widely used Chinese herb. J Ethnopharmacol 263:113216. https://doi.org/10.1016/j.jep.2020.113216
50. Yang R, Li WD, Ma YS, Zhou S, Xue YT, Lin RC, Liu Y (2017) The molecular identification of licorice species and the quality evaluation of licorice slices. Acta Pharm Sin 52:318-326. https://doi.org/10.16438/j.0513-4870.2016-0602
51. Yang WJ, Du YT, Zhou YB, Chen J, Xu ZS, Ma YZ, Chen M, Min DH (2019) Overexpression of TaCOMT Improves Melatonin Production and Enhances Drought Tolerance in Transgenic Arabidopsis. Int J Mol Sci 20:10.3390/ijms20030652
52. Yi Y, Li JH, Lai XY, Zhang M, Kuang Y, Bao YO, Yu R, Hong W, Muturi E, Xue H, Wei HP, Li T, Zhuang H, Qiao X, Xiang KH, Yang H, Ye M (2022) Natural triterpenoids from licorice potently inhibit SARS-CoV-2 infection. J Adv Res 36:201-210. https://doi.org/10.1016/j.jare.2021.11.012
53. Yin YC, Hou JM, Tian SK, Yang L, Zhang ZX, Li WD, Liu Y (2020) Overexpressing chalcone synthase (CHS) gene enhanced flavonoids accumulation in Glycyrrhiza uralensis hairy roots. Bot Lett 167:219-231. https://doi.org/10.1080/23818107.2019.1702896
54. Zeng F, Weng ZB, Zheng HL, Xu MM, Liang XF, Duan JN (2021) Preparation and characterization of active oxidized starch films containing licorice residue extracts and its potential against methicillin-resistant S. aureus. Int J Biol Macromol 187:858-866. https://doi.org/10.1016/j.ijbiomac.2021.07.179
55. Zhang K, Cui HT, Cao SH, Yan L, Li MN, Sun Y (2019) Overexpression of CrCOMT from Carex rigescens increases salt stress and modulates melatonin synthesis in Arabidopsis thaliana. Plant Cell Rep 38:1501-1514. https://doi.org/10.1007/s00299-019-02461-7
56. Zhang N, Ma XM, Li R, Xue YH, Sun YS, Nie SS, Zhang LG (2019) Transcriptome-based analysis of carotenoid accumulation-related gene expression in petals of Chinese cabbage (Brassica rapa L.). 3 Biotech 9:274. https://doi.org/10.1007/s13205-019-1813-6
57. Zhang RX, Sun Y, Su JP, Wang SJ, Tong H, Liu YQ, Sun LJ (2021) Research Progress on Plant Melatonin. Current Biotechnology 11:297-303. https://doi.org/10.19586/j.2095-2341.2020.0148

Zhou W, Yang S, Zhang Q, Xiao RY, Li B, Wang DH, Niu JF, Wang SQ, Wang ZZ (2021) Functional Characterization of Serotonin N-Acetyltransferase Genes (SNAT1/2) in Melatonin Biosynthesis of Hypericum perforatum. Front Plant Sci 12:781717. https://doi.org/10.3389/fpls.2021.781717

Tables

Table 1 Mutation sites in COMT sequences in *COMT*⁻ hairy root samples

Samples	Registered sequence MZ169549 in GenBank	Sequencing results	Mutation sites	Synonymous / Missense mutations
COMT-2	~NNAYGMT~	~NNAYGMT~	None	Synonymous (S)
COMT-5	~LPFN~	~LP.	160	Missense (M)
COMT-6	~AYGMTAF~	~AYGTTAF~	174	M
COMT-8	~VGSVVDVG~	~VGSVADVG~	219	M

Note: The editing sites are marked in red; ~ represents the abbreviated amino acid sequences without mutations

Table 2 Mutation sites in CRTZ sequences in *CRTZ*⁻ hairy root samples

Samples	Registry sequence MZ169550 in GenBank	Sequencing results	Mutation sites	Synonymous / Missense mutations
CRTZ-1	~INAAPAITLLS~	~INAVPAIALLS~	200	M
CRTZ-5-2			204	
CRTZ-6				
CRTZ-8-1				
CRTZ-2-1	~INAAPA~	~INAVPA~	200	M
CRTZ-2-2	~HESHH~	~HEPHH~	179	M
	~INAAPA~	~NAVPA~	200	
CRTZ-3	~PAITLLS~	~PAIALLS~	204	M
CRTZ-4				
CRTZ-5-1				
CRTZ-7-1				
CRTZ-7-2				
CRTZ-8-2				

Note: The editing sites are marked in red; ~ represents the abbreviated amino acid sequences without mutations

Table 3 Mutation sites in F3'H sequences in *F3'H* hairy root samples

Samples	Registered sequence MZ169551 in GenBank	Sequencing results	Mutation sites	Synony / Misse mutatic
F3’H-2	MMGRRVFDDGSGSCDPRADE	MIGRRVFDDGNGGCDPRADEFK	2/11/13/30/43/56/59/60/64/	M
F3’H-4-1	FKAMVVELMVLGGVFNISDFIPQLA	AMVVELMALGGVFNISDFIPPLAWLDLQGVQ	69/76/78/79/81/96/100	
F3’H-5-1	LDLQGVQAKVKKVEKKFHAFLTNIIEEHKSS	AKIKKLYKKFDAFLTSIIEEHKNSNYKSGEHKDLLTA		
F3’H-10	ISKGGEHKDLLTALLSHVGVPDENG~	LLSHVEVPDDNG~		
F3’H-4-2	77~ISKGGEH~	77~ISKGGEH~	None	S
F3’H-5-2	52~QAKVKK	52~QAKIKK	56	M
F3’H-7				
F3’H-9-1				
F3’H-8	MMGRRVFDDGSGSCDPRADEFKA	MIGRRVFDDGNGGCDPRADEFKAMVVE	2/11/13/30/43/56/57/59/60/	M
	MVVELMVLGGVFNISDFIPQLAWLDLQ	LMALGGVFNISDFIPPLAWLDLQGVQAKIT	64/65/69/76/78/79/81/96/100	
	GVQAKIKKVEKKFHAFLTNIIEEHKSSISKG	KLYKKFDVFLTSIIEEHKNSNYKSGEHKDLLT		
	GEHKDLLTALLSHVGVPDENG~	ALLSHVEVPDDNG~		
F3’H-9-2	MMGRRVFDDGSGSCDPRADEFKAMVVELMV	MIGRRVFDDGNGGCDPRADEF	2/11/13/30/43/56/57/59/60/	M
	LGGVFNISDFIPQLAWLDLQGVQA	KAMVVELMALGGVFNISDFIPPLAW	64/69/76/78/79/81/96/100	
	KIKKVEKKFHAFLTNIIEEHKSSISKG	LDLQGVQAKITKLYKKFDAFLTSIIEEH		
	GEHKDLLTALLSHVGVPDENG~	KNSNYKSGEHKDLLTALLSHVEVPDDNG~		

Note: The editing sites are marked in red; ~ represents the abbreviated amino acid sequences without mutations

Table 4 GA contents in all the *G. uralensis* hairy root samples

Groups	Lines	Repetition	Peak area (mAU*s)	Content ($mg \cdot g^{-1}$)	Average GA content ($mg \cdot g^{-1}$)	Ratio (WT vs other groups)
Wild Type	WT	1	15622	3.2201	3.3242	1.0000
		2	16691	3.4193		
		3	16230	3.3334		
Negative Control	NC-PCA	1	14922	3.0897	3.5188	1.0585
		2	21123	4.2451		
		3	15629	3.2214		
	NC-PHSE	1	15979	3.2867	3.3459	1.0065
		2	15581	3.2125		
		3	17331	3.5386		
F3'H Overexpression	$F3'H^+$-1	1	9816	2.1383	2.3654	1.4053
		2	13362	2.7990		
		3	12142	2.5717		
	$F3'H^+$-3	1	12866	2.7066		
		2	10307	2.2298		
		3	10156	2.2017		
	$F3'H^+$-4	1	13390	2.8043		
		2	12061	2.5566		
		3	7804	1.7634		
	$F3'H^+$-5	1	11337	2.4217		
		2	12902	2.7133		
		3	10563	2.2775		
	$F3'H^+$-6	1	10863	2.3334		
		2	12745	2.6841		
		3	12416	2.6228		
	$F3'H^+$-7	1	11091	2.3759		
		2	11883	2.5235		
		3	7338	1.6766		
	$F3'H^+$-10	1	9349	2.3211		
		2	9255	2.7905		
		3	10088	3.1268		
F3'H Knockout	$F3'H^-$-2	1	35235	2.0513	5.4744	0.6072
		2	34542	2.0338		
		3	28047	2.1890		
	$F3'H^-$-7	1	22062	6.8746		
		2	20175	6.7454		
		3	18266	5.5352		
	$F3'H^-$-8	1	29807	4.4201		
		2	32511	4.0685		
		3	32037	3.7128		
	$F3'H^-$-10	1	33682	6.5852		

		2	28785	5.6728		
		3	17497	3.5695		
CRTZ Overexpression	$CRTZ^{+}$-1	1	7689	1.7420	2.2050	1.5076
		2	11439	2.4407		
		3	10363	2.2402		
	$CRTZ^{+}$-2	1	11490	2.4502		
		2	10467	2.2596		
		3	9033	1.9924		
	$CRTZ^{+}$-3	1	8364	1.8678		
		2	8699	1.9302		
		3	8394	1.8734		
	$CRTZ^{+}$-4	1	12744	2.6839		
		2	13702	2.8624		
		3	13387	2.8037		
	$CRTZ^{+}$-5	1	5286	1.2943		
		2	9964	2.1659		
		3	11588	2.4685		
CRTZ Knockout	$CRTZ^{-}$-1	1	47746	9.2057	5.3651	0.6196
		2	33414	6.5353		
		3	22832	4.5636		
	$CRTZ^{-}$-3	1	18038	3.6703		
		2	17668	3.6014		
		3	22571	4.5149		
	$CRTZ^{-}$-4	1	20373	4.1054		
		2	21915	4.3927		
		3	18838	3.8194		
	$CRTZ^{-}$-6	1	44316	8.5666		
		2	46585	8.9894		
		3	27496	5.4326		
	$CRTZ^{-}$-7	1	15217	3.1447		
		2	15282	3.1568		
		3	35798	6.9795		
COMT Overexpression	$COMT^{+}$-1	1	9958	2.1648	2.3509	1.4140
		2	8792	1.9475		
		3	10341	2.2361		
	$COMT^{+}$-4	1	9819	2.1389		
		2	11851	2.5175		
		3	9984	2.1696		
	$COMT^{+}$-7	1	12220	2.5862		
		2	13024	2.7361		
		3	14912	3.0878		
	$COMT^{+}$-10	1	13328	2.7927		

		2	9653	2.1079		
		3	8580	1.9080		
	$COMT^{+}$-11	1	9961	2.1653		
		2	11810	2.5099		
		3	10118	2.1946		
COMT Knockout	$COMT^{-}$-5	1	24364	4.8490	4.2746	0.7777
		2	23633	4.7128		
		3	23436	4.6761		
	$COMT^{-}$-6	1	25829	5.1220		
		2	21247	4.2682		
		3	15636	3.2227		
	$COMT^{-}$-8	1	23274	3.0180		
		2	17623	3.7092		
		3	13988	4.8933		

Figures

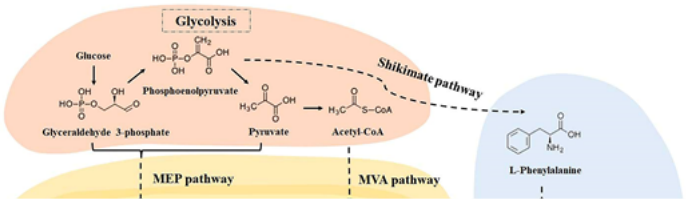

Figure 1

Metabolic pathways in *G. uralensis*

Glycolysis, the primary metabolic pathway, is marked in orange, the terpenoids metabolic pathway is marked in yellow, and the phenlpropanoids metabolic pathway for flavonoids synthesis is marked in blue. The primary metabolites, such as pyruvate, acetyl-CoA, and phosphoenolpyruvate, flow into different pathways to produce various secondary metabolites. CRTZ, COMT, and F3'H are key enzymes involved in the MEP pathway, monolignols biosynthetic pathway, and flavonols biosynthetic pathway, respectively. Their regulatory effects on the biosynthesis of GA are far from clear. The dotted arrows indicate multi-step reaction, and the straight arrows indicate single-step reaction. MEP, 2-C-methl-D-erythritol-4-phospate; MVA, Mevalonate; DMAPP, Dimethylallyl diphosphate; IPP, Isopentenyl pyrophosphate; IDI, Isopentenyl diphosphate isomerase; CRTZ, Beta-carotene 3-hydroxylase; F3'H, Flavonoid 3'-monooxygenase; COMT, Caffeic acid 3-O-methyltransferase

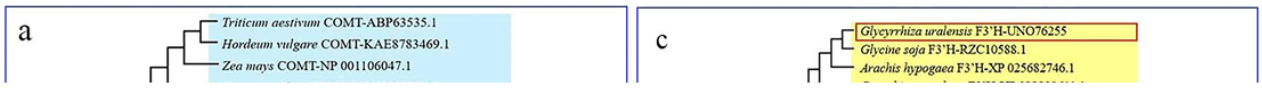

Figure 2

The phylogenetic trees of COMT (a), CRTZ (b), and F3'H (c)

Species from Monocotyledoneae, Dicotyledoneae, Pteridophyta, and Bryophyta are marked in blue, yellow, red, and green, respectively. The target COMT, CRTZ, and F3'H orthologs identified from *G. uralensis* are marked in red boxes. The outgroups are marked in gray

Figure 3

The induction and culture of *G. uralensis* hairy roots

The photos of 10-, 20-, and 30-day old hairy root lines after the onset of induction in solid medium. WT represents wild type hairy roots, NC-PCA represents the negative control hairy roots containing vector pCAMBIA1305.1, NC-PHSE represents the negative control hairy roots containing vector pHSE401, *F3'H*, *COMT*,

and *CRTZ*$^{-}$ represent hairy root lines knocking out *F3'H*, *COMT*, and *CRTZ*, respectively, and *F3'H*$^{+}$, *COMT*$^{+}$, and *CRTZ*$^{+}$ represent hairy root lines overexpressing *F3'H*, *COMT*, and *CRTZ*, respectively

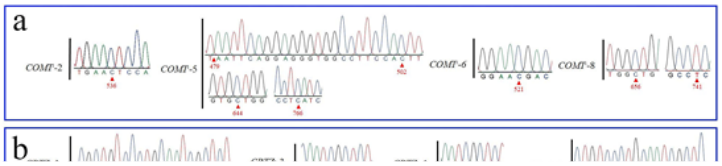

Figure 4

Characterization of gene knockout and overexpression in transgenic *G. uralensis* hairy root lines

a, b, and **c** show the homozygous mutations in hairy root lines *CRTZ*$^{-}$, *COMT*$^{-}$, and *F3'H*$^{-}$, respectively. The mutation sites are marked by the red triangles located below peaks. **d** shows the relative expression levels of the three target genes in hairy root lines *F3'H*$^{+}$, *COMT*$^{+}$, and *CRTZ*$^{+}$. * represents $P < 0.05$ (vs. WT)

Figure 5

UPLC sample preparation

a shows the 3-week old hairy root lines cultured in liquid medium. **b** shows the hairy root lines collected for UPLC sample preparation. WT represents wild type hairy roots, NC-PCA represents the negative control hairy roots containing vector pCAMBIA1305.1, NC-PHSE represents the negative control hairy roots containing vector pHSE401, *F3'H*$^{-}$, *COMT*$^{-}$, and *CRTZ*$^{-}$ represent hairy root lines knocking out *F3'H*, *COMT*, and *CRTZ*, respectively, and *F3'H*$^{+}$, *COMT*$^{+}$, and *CRTZ*$^{+}$ represent hairy root lines overexpressing *F3'H*, *COMT*, and *CRTZ*, respectively

Figure 6

The GA contents in *G. uralensis* hairy root samples

a shows UPLC chromatograms, line 1 is for GA reference substance, lines 2~10 are for sample WT, NC-PCA, NC-PHSE, *F3'H*$^{+}$, *COMT*$^{+}$, *CRTZ*$^{+}$, *F3'H*$^{-}$, *COMT*$^{-}$, and *CRTZ*$^{-}$, respectively. **b** shows the GA content in each hairy root sample. **c** shows the GA content among tested groups. * represents $P < 0.05$ (vs. WT). $^{\#}$ represents $P < 0.05$ (vs. negative control NC-PCA or NC-PHSE)

Supplementary Files

This is a list of supplementary files associated with this preprint. Click to download.

- Supplementalmaterials.docx